

Luis C. Ho² and John Kormendy³

1. SUPERMASSIVE BLACK HOLES AND THE AGN PARADIGM

Quasars are among the most energetic objects in the Universe. We now know that they live at the centers of galaxies and that they are the most dramatic manifestation of the more general phenomenon of active galactic nuclei (AGNs). These include a wide variety of exotica such as Seyfert galaxies, radio galaxies, and BL Lacertae objects. Since the discovery of quasars in 1963, much effort has gone into understanding their energy source. The suite of proposed ideas has ranged from the relatively prosaic, such as bursts of star formation that make multiple supernova explosions, to the decidedly more colorful, such as supermassive stars, giant pulsars or “spinars,” and supermassive black holes (hereinafter BHs). Over time, BHs have gained the widest acceptance. The key observations that led to this consensus are as follows.

Quasars have prodigious luminosities. Not uncommonly, $L \sim 10^{46}$ erg s⁻¹; this is 10 times the luminosity of the brightest galaxies. Yet they are tiny, because they vary on timescales of hours. From the beginning, the need for an extremely compact and efficient engine could hardly have been more apparent. Gravity was implicated, because collapse to a black hole is the most efficient energy source known. The most cogent argument is due to Donald Lynden-Bell (1969, *Nature*, **223**, 690). He showed that any attempt to power quasars by nuclear reactions alone is implausible. First, a lower limit to the total energy output of a quasar is the energy, $\sim 10^{61}$ erg, that is stored in its radio-emitting plasma halo. This energy weighs 10^{40} g or $10^7 M_{\odot}$. But nuclear reactions produce energy with an efficiency of only $\epsilon = 0.7\%$. Then the waste mass left behind in powering quasars would be at least $M_{\bullet} \simeq 10^9 M_{\odot}$. Lynden-Bell argued further that quasar engines are $2R \lesssim 10^{15}$ cm in diameter because large variations in quasar luminosities are observed on timescales as short as 10 h. But the gravitational potential energy of $10^9 M_{\odot}$ compressed into a volume as small as 10 light hours is $\sim GM_{\bullet}^2/R \gtrsim 10^{62}$ erg. As Lynden-Bell noted, “Evidently although our aim was to produce a model based on nuclear fuel, we have ended up with a model which has produced more than enough energy by gravitational contraction. The nuclear fuel has ended as an irrelevance.” We now know that the total energy output is larger than the energy that is stored in a quasar’s radio source; this strengthens the argument. Meanwhile, a caveat has appeared: the objects that vary most rapidly are now thought to contain relativistic jets that are beamed at us. This boosts the power of a possibly small part of the quasar engine and weakens the argument that the object cannot vary on timescales less than the light travel time across it. But this phenomenon would not occur at all if relativistic motions were not involved, so BH-like potential wells are still implicated. These considerations suggest that quasar power derives from gravity.

¹ To appear in *Encyclopedia of Astronomy and Astrophysics*

² Carnegie Observatories, 813 Santa Barbara St., Pasadena, CA 91101-1292

³ Department of Astronomy, RLM 15.308, University of Texas, Austin, TX 78712-1083

The presence of deep gravitational potentials has long been inferred from the large velocity widths of the emission lines seen in optical and ultraviolet spectra of AGNs. These are typically 2000 to 10,000 km s⁻¹. If the large Doppler shifts arise from gravitationally bound gas, then the binding objects are both massive and compact. The obstacle to secure interpretation has always been the realization that gas is easy to push around: explosions and ejection of gas are common astrophysical phenomena. The observation that unambiguously points to relativistically deep gravitational potential wells is the detection of radio jets with plasma knots that are seen to move faster than the speed of light, c . Apparent expansion rates of $1 - 10 c$ are easily achieved if the true expansion rate approaches c and the jet is pointed almost at us.

The final pillar on which the BH paradigm is based is the observation that many AGN jets are well collimated and straight. Evidently AGN engines can remember ejection directions with precision for up to 10⁷ yr. The natural explanation is a single rotating body that acts as a stable gyroscope. Alternative AGN engines that are made of many bodies – like stars and supernovae – do not easily make straight jets.

A variety of other evidence also is consistent with the BH picture, but the above arguments were the ones that persuaded a majority of the astronomical community to take the extreme step of adopting BHs as the probable engine for AGN activity. In the meantime, BH alternatives such as single supermassive stars and spinars were shown to be dynamically unstable and hence short-lived. Even if such objects can form, they are believed to collapse to BHs.

The above picture became paradigm long before there was direct evidence for BHs. Dynamical evidence is the subject of the present and following articles. Meanwhile, there are new kinds of observations that point directly to BH engines. In particular, recent observations by the *Advanced Satellite for Cosmology and Astrophysics* (ASCA) have provided strong evidence for relativistic motions in AGNs. The X-ray spectra of many Seyfert galaxy nuclei contain iron K α emission lines (rest energies of 6.4 – 6.9 keV; see Figure 1). These lines show enormous Doppler broadening — in some cases approaching 100,000 km s⁻¹ or 0.3 c — as well as asymmetric line profiles that are consistent with relativistic boosting and dimming in the approaching and receding parts, respectively, of BH accretion disks as small as a few Schwarzschild radii.

The foregoing discussion applies to the most powerful members of the AGN family, namely quasars and high-luminosity Seyfert and radio galaxies. It is less compelling for the more abundant low-luminous objects, where energy requirements are less demanding and where long jets or superluminal motions are seen less frequently or less clearly. Therefore a small but vocal competing school of thought continues to argue that stellar processes alone, particularly those that occur during bursts of star formation, can reproduce many AGN characteristics. Nonetheless, dynamical evidence suggests that BHs *do* lurk in some mildly active nuclei, and, as discussed in the next article, even in the majority of inactive galaxies.

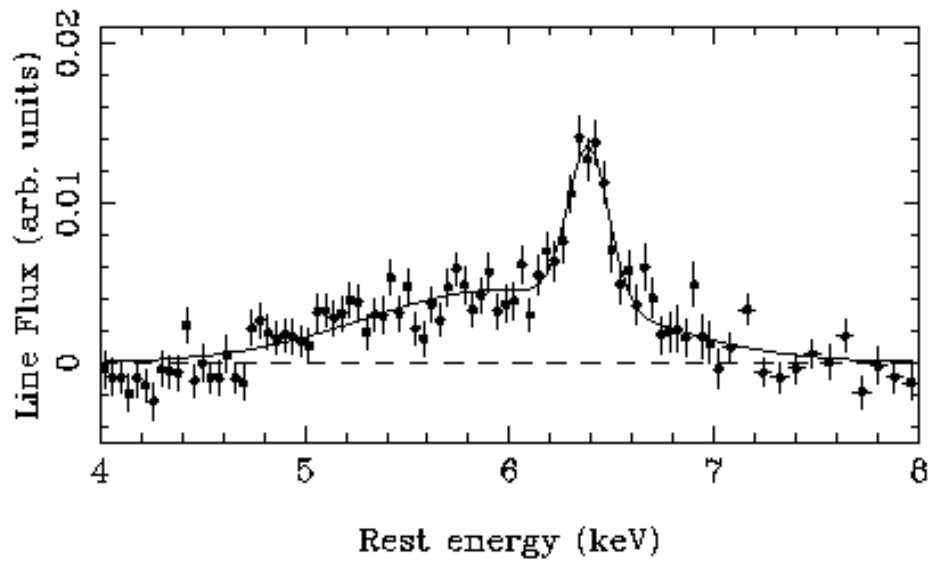


Figure 1. A composite x-ray spectrum of Seyfert nuclei taken with *ASCA* showing the relativistically broadened Fe K α line. The solid line is a fit to the line profile using two Gaussians, a narrow component centered at 6.4 keV and a much broader, redshifted component. [Figure adapted from Nandra, K., *et al. Astrophys. J.* **477**, 602 (1997).]

2. MEASURING AGN MASSES: DIRECT METHODS

Very general arguments suggest that quasar engines have masses $M_{\bullet} \sim 10^6$ to $10^9 M_{\odot}$. Gravitational collapse is believed to liberate energy with an efficiency of $\epsilon \simeq 0.1$; Lynden-Bell's arguments then imply that typical remnant masses are $M_{\bullet} \sim 10^8 M_{\odot}$. Better estimates can be derived by asking what we need in order to power quasar luminosities, which range from 10^{44} to $10^{47} \text{ erg s}^{-1}$ or 10^{11} to $10^{14} L_{\odot}$. For $\epsilon = 0.1$, the engine must consume 0.02 to $20 M_{\odot} \text{ yr}^{-1}$. How much waste mass accumulates depends on how long quasars live. This is poorly known. If they live long enough to make radio jets that are collimated over several Mpc, and if their lifetimes are conservatively estimated as the light travel time along the jets, then quasars last $\gtrsim 10^7$ yr and reach masses $M_{\bullet} \gtrsim 10^5$ to $10^8 M_{\odot}$. But the most rigorous lower limit on M_{\bullet} follows from the condition that the outward force of radiation pressure on accreting matter not overwhelm the inward gravitational attraction of the engine, a condition which, admittedly, strictly holds only if the accreting material and the radiation have spherical symmetry. This so-called Eddington limit requires that $L \leq L_E \equiv (4\pi G c m_p / \sigma_T) M_{\bullet} = 1.3 \times 10^{38} (M_{\bullet} / M_{\odot}) \text{ erg s}^{-1}$, or equivalently that $M_{\bullet} \geq 8 \times 10^5 (L / 10^{44} \text{ erg s}^{-1}) M_{\odot}$. Here G is the gravitational constant, m_p is the mass of the proton, and σ_T is the Thompson cross section for electron scattering. We conclude that we are looking for BHs with masses $M_{\bullet} \sim 10^6$ to $10^9 M_{\odot}$. Finding them has become one of the “Holy Grails” of astronomy because of the importance of confirming or disproving the AGN paradigm.

AGNs provide the impetus to look for BHs, but active galaxies are the most challenging hunting ground. Stellar dynamical searches first found central dark objects in inactive galaxies (see the next article), but they cannot be applied in very active galaxies, because the nonthermal

nucleus outshines the star light. We can estimate masses using the kinematics of gas, but only if it is unperturbed by nongravitational forces. Fortunately, this complication can be ruled out *a posteriori* if we observe that the gas is in Keplerian rotation around the center, i. e., if its rotation velocity as a function of radius is $V(r) \propto r^{-1/2}$. We can also stack the cards in our favor by targeting galaxies that are only weakly active and that appear to show gas disks in images taken through narrow bandpasses centered on prominent emission lines.

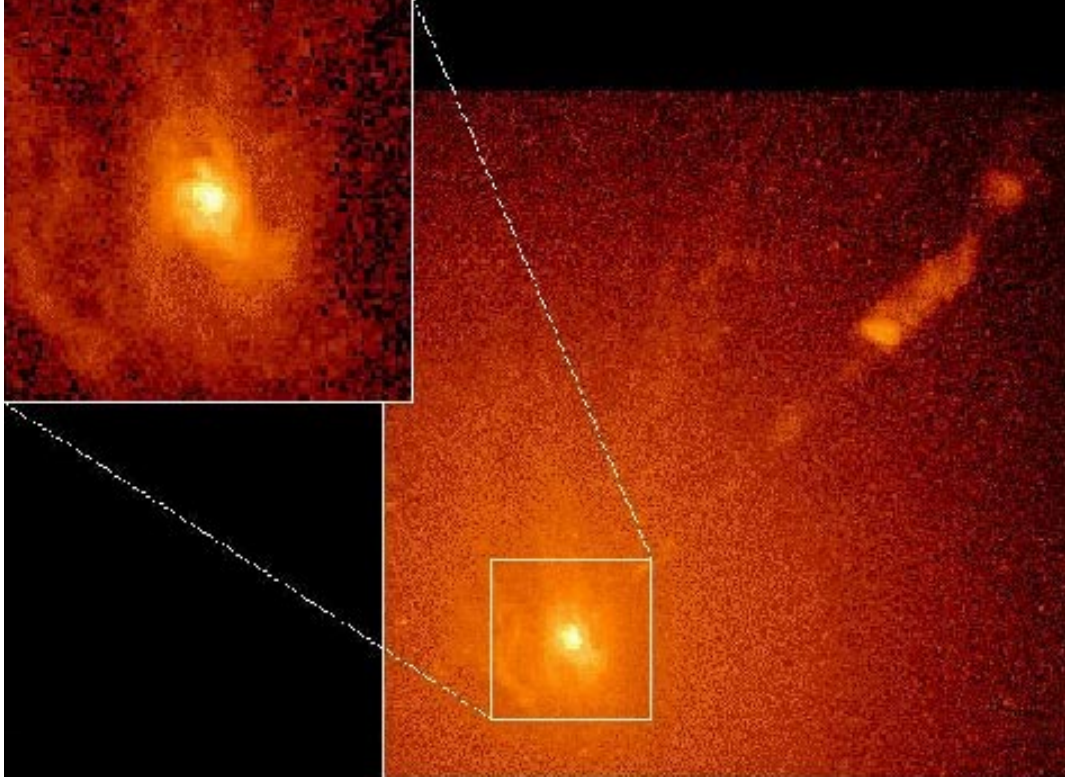


Figure 2a. *HST* image of the ionized gas disk near the center of the giant elliptical galaxy M87. The data were taken with the Second Wide Field/Planetary Camera through a filter that isolates the optical emission lines $H\alpha$ and $[N II] \lambda\lambda 6548, 6583$. The left inset is an expanded view of the gas disk; for an adopted distance of 16.8 Mpc, the region shown is $5'' \times 5''$ or 410×410 pc. The disk has a major axis diameter of ~ 150 pc, and it is oriented perpendicular to the optical jet. [Image courtesy of NASA/Space Telescope Science Institute, based on data originally published by Ford, H. C., *et al. Astrophys. J.* **435**, L27 (1994).]

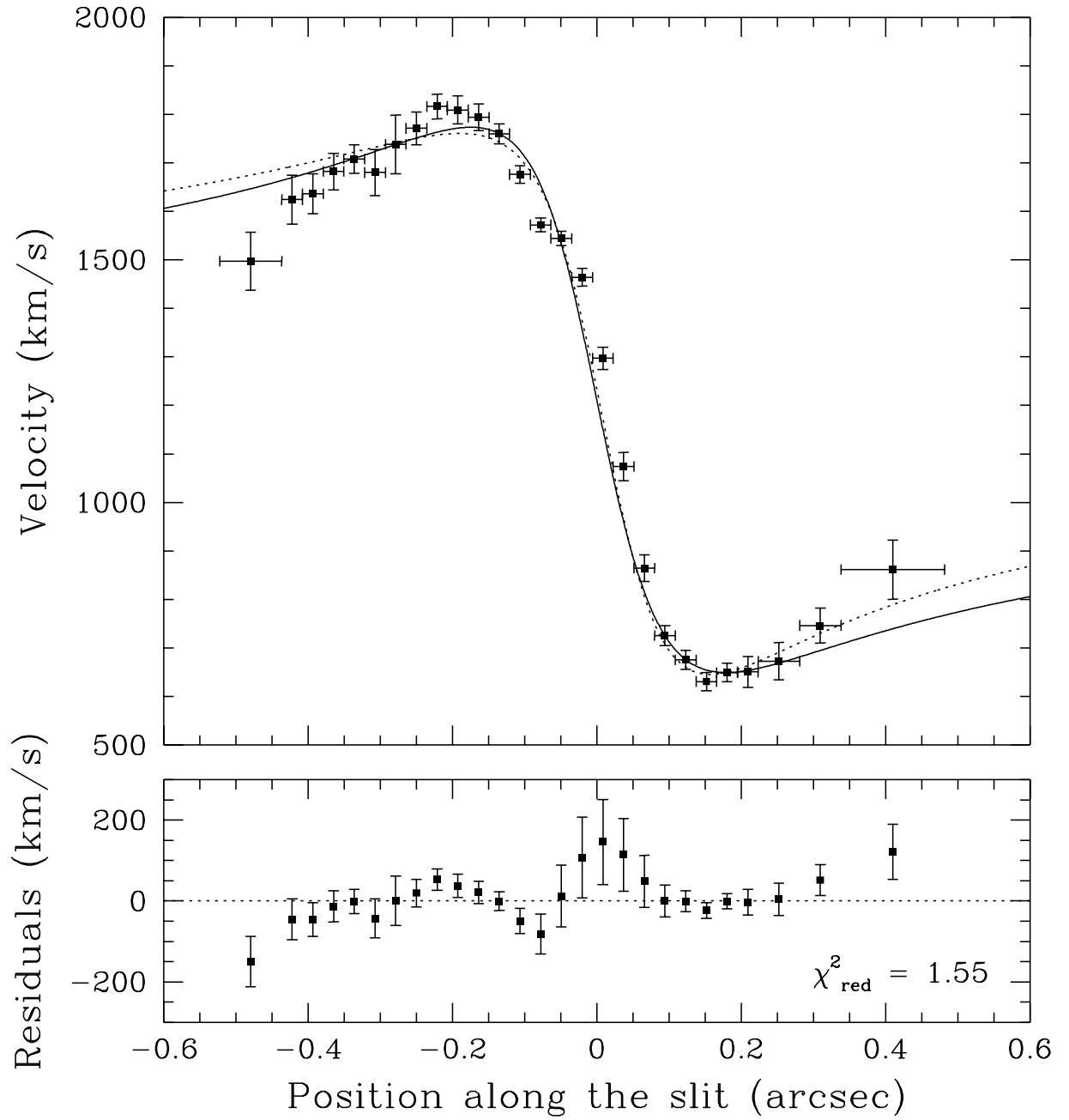


Figure 2b. Optical emission-line rotation curve for the nuclear disk in M87. The data were taken with the Faint Object Camera on *HST*. The curves in the upper panel correspond to two different Keplerian thin disk models, and the bottom panel shows the residuals for the best-fitting model. [Figure adapted from Macchetto, F., *et al. Astrophys. J.* **489**, 579 (1997).]

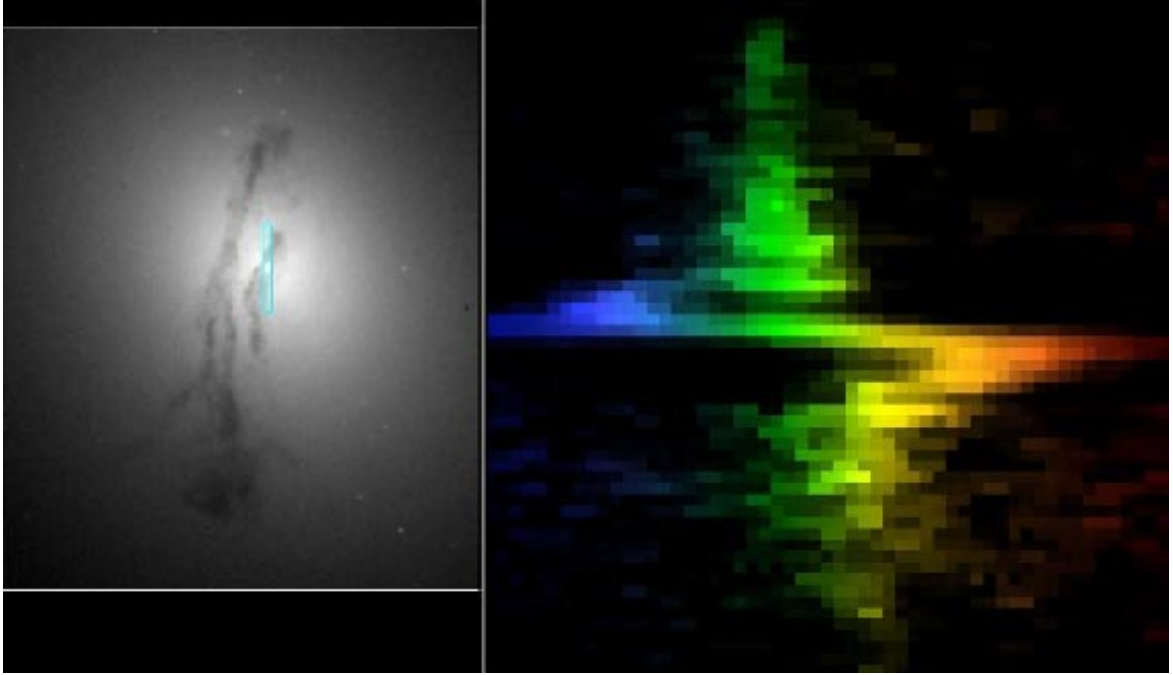


Figure 3. (*Left*) *HST* image of the central region of the giant elliptical galaxy M84; the box measures $22'' \times 19''$ or $1.8 \text{ kpc} \times 1.6 \text{ kpc}$ for an adopted distance of 16.8 Mpc. The data were taken with the Second Wide Field/Planetary Camera through a filter that isolates the optical emission lines $\text{H}\alpha$ and $[\text{N II}] \lambda\lambda 6548, 6583$. The slit of the Space Telescope Imaging Spectrograph was placed along the major axis of the nuclear gas disk (blue rectangle). (*Right*) Resulting spectrum of the central $3''$ (240 pc). The abscissa is velocity and the ordinate is distance along the major axis. The spectrum shows the characteristic kinematic signature of a rotating disk. The velocity scale is coded such that blue and red correspond to blue and red shifts, respectively; the total velocity range is 1445 km s^{-1} . [Image courtesy of NASA/Space Telescope Science Institute, based on data originally published by Bower, G. A., *et al. Astrophys. J. Lett.* **483**, L33 (1997) and Bower, G. A., *et al. Astrophys. J. Lett.* **492**, L111 (1998).]

2.1 Kinematics of Optical Emission Lines

High-resolution optical images taken with ground-based telescopes and especially with the *Hubble Space Telescope* (*HST*) show that many giant elliptical galaxies contain nuclear disks of dust and ionized gas. The most famous case is M87 (Figure 2a). The disk measures ~ 150 pc across, and its rotation axis is closely aligned with the optical and radio jet. This is in accord with the BH accretion picture. The disk is in Keplerian rotation (Figure 2b) around an object of mass $M_{\bullet} \simeq 3 \times 10^9 M_{\odot}$. Furthermore, this object is dark: the measured mass-to-light ratio exceeds 100 in solar units, and this is much larger than that of any known population of stars. Moreover, the dark mass must be very compact: the velocity field limits its radial extent to be less than 5 pc. Therefore its density exceeds $10^7 M_{\odot} \text{ pc}^{-3}$. Another illustration of this technique is given in Figure 3. M84, also a denizen of the Virgo cluster of galaxies, is a twin of M87 in size, and it, too, harbors an inclined nuclear gas disk (diameter ~ 80 pc), whose rotation about the center betrays an invisible mass of $M_{\bullet} \simeq 2 \times 10^9 M_{\odot}$. Other cases are reported (NGC 4261, NGC 6251, NGC 7052), and searches for more are in progress.

2.2 Kinematics of Radio Masers

A related approach exploits the few cases where 22 GHz microwave maser emission from water molecules has been found in edge-on nuclear disks of gas. Particularly strong “megamasers” allow radio astronomers to use interferometry to map the velocity field with exquisite angular resolution. In the most dramatic application of this method, the Very Long Baseline Array was used to achieve resolution $0''.0006$ – 100 times better than that delivered by *HST* – in observations of the Seyfert galaxy NGC 4258. This is only 6 Mpc away, so the linear resolution was a remarkable 0.017 pc. The masers trace out a slightly warped annulus with an inner radius of 0.13 pc, an outer radius of 0.26 pc, and a thickness of < 0.003 pc (Figure 4, *left*). The masers with nearly zero velocity with respect to the galaxy are on the near side of the disk along the line of sight to the center, while the features with high negative (approaching) and positive (receding) velocities come from the disk on either side of the center. High velocities imply that $3.6 \times 10^7 M_{\odot}$ of binding matter resides interior to $r = 0.13$ pc. What is most compelling about NGC 4258 is the observation that the rotation curve is so precisely Keplerian (Figure 4, *right*). From this result, one can show that the radius of the mass distribution must be $r \lesssim 0.012$ pc. If the central mass were *not* a BH, its density would be extraordinarily high, $\rho > 5 \times 10^{12} M_{\odot} \text{ pc}^{-3}$. This is comparable to the density of the dark mass at the center of our Galaxy (see following article). Under these extreme conditions, one can show that a cluster of stellar remnants (white dwarf stars, neutron stars, and stellar-size black holes) or substellar objects (planets and brown dwarfs) are short-lived. Astrophysically, these are the most plausible alternatives to a BH. Therefore the dynamical case for a supermassive black hole is stronger in NGC 4258 and in our Galaxy than in any other object.

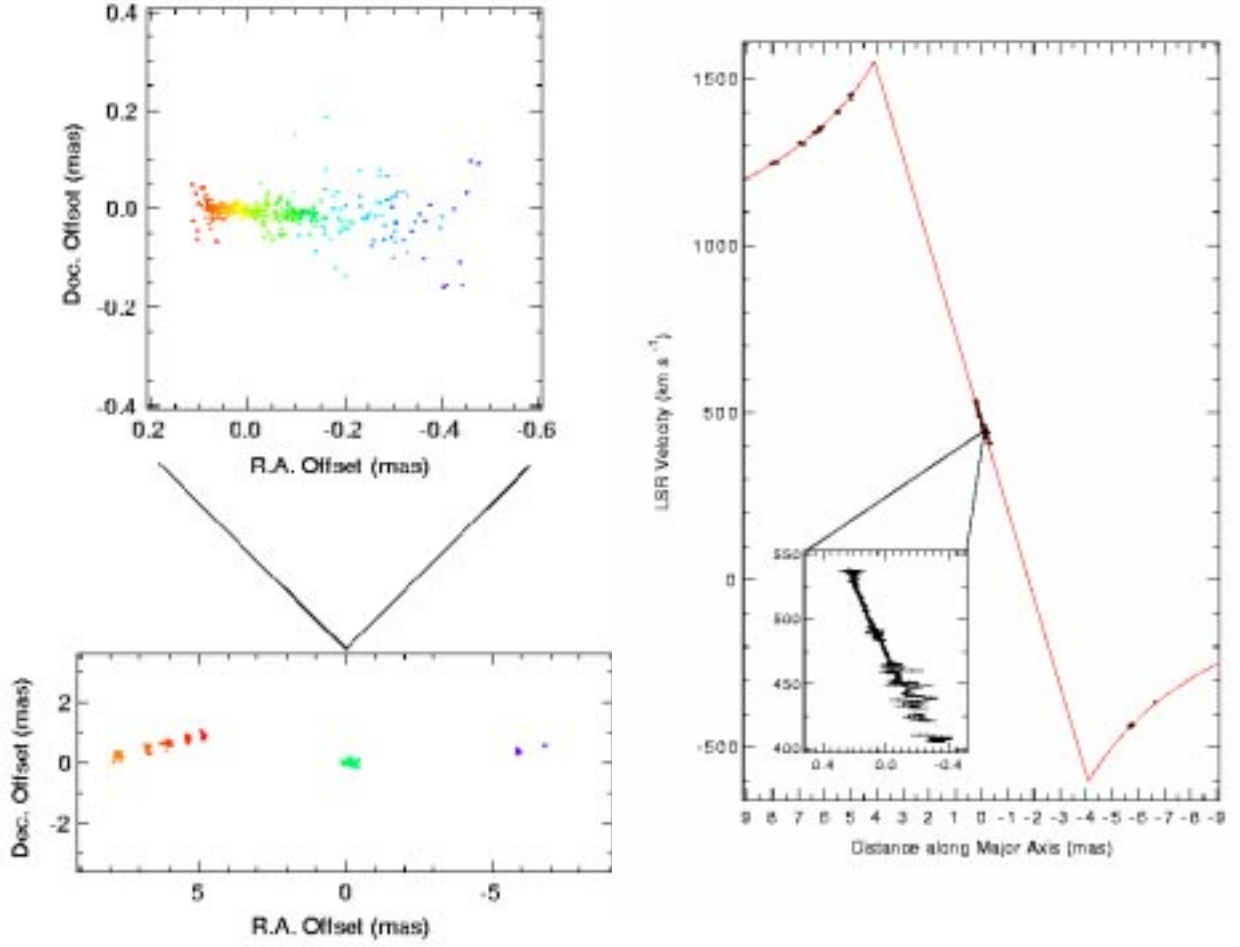


Figure 4. (*Left*) Spatial distribution of the water masers in NGC 4258, color-coded so that blue and red correspond to blueshifted and redshifted velocities, respectively. The maser spots are distributed in a thin, warped annulus that is only 4° from edge-on. For an adopted distance of 6.4 Mpc, 1 mas = 0.031 pc. The top panel shows an expanded view of the emission near the systemic velocity of the galaxy. (*Right*) Light-of-sight velocity as a function of distance along the major axis of the annulus. The high-velocity features are accurately fitted by a Keplerian model, overplotted as a continuous line. The emission near the systemic velocity, magnified in the inset, lies at nearly constant radius in the front part of the disk along the line of sight to the center. The linear velocity gradient results from the change in projection of the rotation velocity. [Figure adapted from Miyoshi, M., *et al.* *Nature* **373**, 127 (1995).]

3. MEASURING AGN MASSES: INDIRECT METHODS

Direct dynamical measurements are impractical for more luminous and more distant AGNs. The tremendous glare from the nucleus outshines the circumnuclear emission from stars, and the violent conditions near the center are likely to subject the gas to nongravitational forces. Indirect methods of estimating central masses have been devised to provide a reality check for these more difficult objects.

3.1 Fitting the Spectra of Accretion Disks

As material falls toward a black hole, it is believed to settle into an accretion disk in which angular momentum is dissipated by viscosity. From the virial theorem, half of the gravitational potential energy U is radiated. Therefore the luminosity is

$$L = \frac{1}{2} \frac{dU}{dt} = \frac{1}{2} \frac{GM_{\bullet} \dot{M}_{\bullet}}{r} . \quad (1)$$

At sufficiently high accretion rates \dot{M}_{\bullet} , the gas is optically thick, and the disk radiates as a thermal blackbody:

$$L = 2\pi r^2 \sigma T^4 . \quad (2)$$

Here $2\pi r^2$ is the surface area of the disk and σ is the Stefan-Boltzmann constant. The effective temperature of the disk as a function of radius r is therefore

$$T(r) \simeq \left(\frac{GM_{\bullet} \dot{M}_{\bullet}}{4\pi \sigma r^3} \right)^{1/4} . \quad (3)$$

Parameterizing the above result in terms of the Eddington accretion rate, $\dot{M}_{\text{E}} \equiv L_{\text{E}}/\epsilon c^2 = 2.2 (\epsilon/0.1)^{-1} (M_{\bullet}/10^8 M_{\odot}) M_{\odot} \text{ yr}^{-1}$, and the Schwarzschild radius, $R_{\text{S}} \equiv 2GM_{\bullet}/c^2 = 2.95 \times 10^{13} (M_{\bullet}/10^8 M_{\odot}) \text{ cm}$, gives

$$T(r) = 6 \times 10^5 \text{ K} \left(\frac{\dot{M}_{\bullet}}{\dot{M}_{\text{E}}} \right)^{1/4} \left(\frac{M_{\bullet}}{10^8 M_{\odot}} \right)^{-1/4} \left(\frac{r}{R_{\text{S}}} \right)^{-3/4} . \quad (4)$$

In other words, the peak of the blackbody spectrum occurs at a frequency of $\nu_{\text{max}} = 2.8 kT/h \simeq 4 \times 10^{16} \text{ Hz}$, where k is Boltzmann's constant and h is Planck's constant. This peak is near 100 \AA or 0.1 keV . In fact, the spectra of many AGNs show a broad emission excess at extreme ultraviolet or soft X-ray wavelengths. This “big blue bump” has often been identified with the thermal emission from the accretion disk. A fit to the luminosity and the central frequency of the big blue bump gives M_{\bullet} and \dot{M}_{\bullet} but not each separately. Corrections for disk inclination and relativistic effects further complicate the analysis. This method is therefore model-dependent and provides only approximate masses. Typical values for quasars are $M_{\bullet} \simeq 10^8 - 10^{9.5} M_{\odot}$ and $\dot{M}_{\bullet} \simeq 0.1 - 1 \dot{M}_{\text{E}}$. Seyfert nuclei appear to have lower masses, $M_{\bullet} \simeq 10^{7.5} - 10^{8.5} M_{\odot}$, and lower accretion rates, $\dot{M}_{\bullet} \simeq 0.01 - 0.5 \dot{M}_{\text{E}}$.

3.2 Virial Masses from Optical Variability

Surrounding the center at a distance of 0.01 to 1 pc from the black hole lies the “broad-line region” (BLR). This is a compact, dense, and highly turbulent swarm of gas clouds or filaments. The clouds are illuminated by the AGN’s photoionizing continuum radiation and reprocess it into emission lines that are broadened to velocities of several thousand km s^{-1} by the strong gravitational field of the black hole. Then

$$M_{\bullet} = \eta \frac{v^2 r_{\text{BLR}}}{G}, \quad (5)$$

where $\eta \simeq 1$ to 3 depends on the kinematic model adopted, v is the velocity dispersion of the gas as reflected in the widths of the emission lines, and r_{BLR} is the radius of the BLR. The latter can be estimated by “reverberation mapping,” as follows. The photoionizing continuum of an AGN typically varies on timescales of days to months. In response, the emission lines vary also, but with a time delay that corresponds to the light travel time between the continuum source and the line-emitting gas. By monitoring the variations in the continuum and the emission lines in an individual object, reverberation mapping provides information on the size of the BLR. These studies also support the assumption that the line widths come predominantly from bound orbital motions. Applying Equation (5) suggests that Seyfert nuclei are powered by black holes with masses $M_{\bullet} \sim 10^7$ to $10^8 M_{\odot}$, while quasar engines are more massive, with $M_{\bullet} \sim 10^8$ to $10^9 M_{\odot}$. Since quasars also live in more massive host galaxies, this supports the emerging correlation (see the following article) between BH mass and the mass of the elliptical-galaxy-like part of the host galaxy.

3.3 X-Ray Variability

Active galactic nuclei vary most conspicuously in hard X-rays (2 – 10 keV). One might hope to use the variability timescale to constrain the size of the X-ray emitting region and hence to estimate the central mass. However, no simple pattern of variability emerges, and defining a meaningful timescale is ambiguous. One approach uses the “fastest doubling time,” Δt , to establish a maximum source size $R \simeq c\Delta t$. High-energy photons presumably come from the hot, inner regions of the accretion disk or in an overlying hot corona. For example, if $R \simeq 5 R_S$, as deduced in some models, we obtain an upper limit to the mass, $M_{\bullet} \lesssim (c^3/10G) \Delta t \sim 10^4 \Delta t M_{\odot}$ (Δt in s). Masses estimated in this way are generally consistent with those obtained from other virial arguments, but they are considerably less robust because of uncertainties in associating the variability timescale with a source size. For example, the x-ray intensity variations could originate from localized “hotspots” in the accretion flow.

X-ray reverberation mapping may in the future be a more powerful tool. The iron $K\alpha$ line is widely believed to be produced by reprocessing of the hard X-ray continuum by the accretion disk. The strikingly large width and skewness of the line profiles (Figure 1), now routinely detected with *ASCA*, reflect the plasma bulk motion within 10 – 100 gravitational radii of the center. The temporal response of the line strength and line profile depends on a number of factors

that, in principle, can be modeled theoretically; these include the geometry of the X-ray source, the structure of the disk, and the assumed (Schwarzschild or Kerr) metric of the black hole. Time-resolved X-ray spectroscopy should become feasible with the *X-ray Multi-Mirror Mission* (*XMM*) in the near future. We can then look forward to constraints both on the masses and the spins of BHs.

4. SUMMARY AND PROSPECTUS

The black hole model for AGN activity has been successful and popular for over three decades. It has withstood the test of time not – at least until recently – because the empirical evidence for BHs has been overwhelming but because the alternatives are so implausible. Now progress has advanced on several fronts. The refurbished *HST* has greatly strengthened the evidence, already growing from ground-based observations, that supermassive dark objects live at the centers of most galaxies. The pace of discoveries is accelerating. The dark objects have exactly the range of masses that we need to explain AGN engines, but we have had no proof that they must be black holes. Then radio interferometry revealed the spectacular maser disk in NGC 4258. For its rotation curve to be as accurately Keplerian as we observe, the central mass must be confined to an astonishingly tiny volume. The inferred density of the central object is so high that astrophysically plausible alternatives can be excluded; a BH is the best explanation. The same conclusion has been reached for the BH candidate at the center of our Galaxy. This is a major conceptual breakthrough.

In addition, *ASCA* has demonstrated that many AGNs show iron emission lines with relativistically broadened profiles. This is arguably the best evidence for the strong gravitational field of a black hole. One of the most interesting prospects for the future is time-resolved X-ray spectroscopy, because hot gas probes closest to an accreting black hole.

Finally, the AGN paradigm can be turned inside-out to give what may prove to be the most direct argument for black holes. BHs were “invented” to explain nuclear activity in galaxies. In recent years, an ironic situation has developed: some BH candidates are too *inactive* for the amount of matter that we believe they are accreting. The same is true of some stellar-mass black hole candidates that accrete gas from evolving companion stars. A number of researchers recently have developed a theory of “advection-dominated accretion” in which the accretion disk cannot radiate most of its energy before it reaches R_S either because it is optically thick or because it is too thin to cool. Unless most of the inflowing material ultimately escapes through an outflow, a possibility being explored, the only way to make the accretion energy disappear is to ensure that the accreting body does not have a hard surface. That is, the *inactivity* of well-fed nuclear engines may be evidence that they have event horizons. Finding event horizons would be definitive proof that AGN engines are black holes.

5. SUGGESTIONS FOR FURTHER READING

- Initial debate concerning the physical nature of quasars is summarized in Burbidge, G., & Burbidge, E. M., *Quasi-Stellar Objects* (San Francisco: Freeman) (1967)

- The three key historical papers that originated the BH hypothesis are
Salpeter, E. E. *Astrophys. J.* **140**, 796 (1964)
Zel'dovich, Ya. B., & Novikov, I. D. *Sov. Phys. Dokl.* **158**, 811 (1964)
Lynden-Bell, D. *Nature* **223**, 690 (1969)
- The argument for “gravity power” was further developed in
Lynden-Bell, D. *Physics Scripta* **17**, 185 (1978)
- Textbook style discussions of AGN physics can be found in
Active Galactic Nuclei, Saas-Fee Course 20, ed. T. J.-L. Courvoisier & M. Mayor (Berlin: Springer) (1990)
Peterson, B. M., *An Introduction to Active Galactic Nuclei* (Cambridge: Cambridge University Press) (1997)
- The BH paradigm is covered at a more technical level in the following review articles:
Rees, M. J. *Ann. Rev. Astr. Astrophys.* **22**, 471 (1984)
Begelman, M. C., Blandford, R. D., & Rees, M. J. *Rev. Mod. Phys.* **56**, 255 (1984)
Blandford, R. D., in *Active Galactic Nuclei, Saas-Fee Course 20*, ed. T. J.-L. Courvoisier & M. Mayor (Berlin: Springer), 161 (1990)
- The search for BHs is reviewed in
Kormendy, J., & Richstone, D. *Ann. Rev. Astr. Astrophys.* **33**, 581 (1995)
Richstone, D., *et al.* *Nature* **395**, A14 (1998)
- The starburst theory for the origin of AGNs has been developed by
Terlevich, R., Tenorio-Tagle, G., Franco, J., & Melnick, J. *M.N.R.A.S.* **255**, 713 (1992)
Terlevich, R., Tenorio-Tagle, G., Rozyczka, M., Franco, J., & Melnick, J. *M.N.R.A.S.* **272**, 198 (1995)
- The following conference proceedings explicitly focus on the observations and interpretation of the more “garden variety” low-luminosity AGNs:
Eracleous, M., Koratkar, A. P., Leitherer, C., & Ho, L. C., eds., *The Physics of LINERs in View of Recent Observations* (San Francisco: Astronomical Society of the Pacific) (1996)
Schmitt, H. R., Kinney, A. L., & Ho, L. C., eds., *The AGN/Normal Galaxy Connection (Advances in Space Research, 23 (5-6))* (Oxford: Elsevier Science Ltd.) (1999)
- Readers interested in a full treatment of the techniques of reverberation mapping should consult
Blandford, R. D., & McKee, C. F. *Astrophys. J.* **255**, 419 (1982)
Peterson, B. M. *Pub. Astr. Soc. Pac.* **105**, 247 (1993)
- Explicit application of reverberation mapping results to derive masses of AGNs was done by
Ho, L. C., in *Observational Evidence for Black Holes in the Universe*, ed. S. K. Chakrabarti (Dordrecht: Kluwer), 157 (1998)

Laor, A. *Astrophys. J. Lett.* **505**, L83 (1998)

- Mass determinations using optical emission-line rotation curves include
Harms, R. J., *et al.* *Astrophys. J. Lett.* **435**, L35 (1994)
Macchetto, F., Marconi, A., Axon, D. J., Capetti, A., Sparks, W. B., & Crane, P. *Astrophys. J.* **489**, 579 (1997)
Bower, G. A., *et al.* *Astrophys. J. Lett.* **492**, L111 (1998)
- The water maser observations of NGC 4258 are described in
Watson, W. D., & Wallin, B. K. *Astrophys. J. Lett.* **432**, L35 (1994)
Miyoshi, M., Moran, J., Herrnstein, J., Greenhill, L., Nakai, N., Diamond, P., & Inoue, M. *Nature* **373**, 127 (1995)
- Arguments against compact dark star clusters in NGC 4258 and the Galaxy are presented in
Maoz, E. *Astrophys. J. Lett.* **494**, L181 (1998)
- These papers discuss the derivation of M_{\bullet} and \dot{M}_{\bullet} by fitting spectra with accretion disk models:
Wandel, A., & Petrosian, V. *Astrophys. J. Lett.* **329**, L11 (1988)
Laor, A. *M.N.R.A.S.* **246**, 369 (1990)
- Attempts to derive masses using X-ray variability have been made by
Wandel, A., & Mushotzky, R. F. *Astrophys. J. Lett.* **306**, L61 (1986)
- The prediction, discovery, and routine detection of broad Fe K α emission lines are described, respectively, in
Fabian, A. C., Rees, M. J., Stella, L., & White, N. E. *M.N.R.A.S.* **238**, 729 (1989)
Tanaka, Y., *et al.* *Nature* **375**, 659 (1995)
Nandra, K., George, I. M., Mushotzky, R. F., Turner, T. J., & Yaqoob, T. *Astrophys. J.* **477**, 602 (1997)
- Prospects for X-ray reverberation mapping are foreseen in
Stella, L. *Nature* **344**, 747 (1990)
Reynolds, C. S., Young, A. J., Begelman, M. C., & Fabian, A. C. *Astrophys. J.* **514**, 164 (1999)
- Advection-dominated accretion is reviewed in
Narayan, R., Mahadevan, R., & Quataert, E., in *The Theory of Black Hole Accretion Discs*, ed. M. A. Abramowicz, G. Björnsson, & J. E. Pringle (Cambridge: Cambridge University Press), 148 (1998)
Mineshige, S., & Manmoto, T., *Advances in Space Research*, **23** (5-6), 1065 (1999)
Blandford, R. D., & Begelman, M. C. *M.N.R.A.S.* **303**, L1 (1999)